



Pergamon

Available online at www.sciencedirect.com

SCIENCE @ DIRECT®



Acta Materialia 51 (2003) 1755–1765

www.actamat-journals.com

Effects of topology on abnormal grain growth in silicon steel

N. Chen ^{a,*}, S. Zaefferer ^a, L. Lahn ^b, K. Günther ^b, D. Raabe ^a

^a Max-Planck-Institut für Eisenforschung, Max-Planck-Str. 1, D-40237 Düsseldorf, Germany

^b ThyssenKrupp Electrical Steel R&D Department, Kurt-Schumacher-Str. 95, D-45881 Gelsenkirchen, Germany

Received 26 July 2002; received in revised form 7 November 2002; accepted 30 November 2002

Abstract

This work addresses the role of grain topology on abnormal grain growth in silicon steel. The question was investigated whether the abnormal grain growth of Goss grains during secondary recrystallization can be interpreted in terms of an initial size advantage that these grains inherit from rolling and primary recrystallization. For this purpose the correlation between crystallographic orientation, size and number of next neighbors of large grains in the subsurface layer of a primary recrystallized silicon steel sheet was investigated. It was found that most of the large grains have an orientation on the η -fiber ($\langle 001 \rangle$ axis parallel to the rolling direction) but are not particularly close to the Goss orientation. Also, no tendency of grains to be larger the closer they are to the Goss orientation was visible. Rather it was found that the scatter of the angular deviation to the Goss orientation is similar over a large range of grain sizes and this was found to be true too if the number of next neighbors of a grain rather than its grain size was checked. One single grain, however, was found that was close to the Goss orientation and had a high number of next neighbors and might therefore act as a nucleus for secondary recrystallization. Nevertheless, grains with a similarly high number of neighbors and a large deviation to the Goss orientation were found, too. Thus, a topological reason for the Goss texture evolution could not yet be proved. However, it might be that the extreme rareness of Goss nuclei (1 out of 10^6 grains) has prevented, up to now, from observing a true nucleus.

© 2003 Acta Materialia Inc. Published by Elsevier Science Ltd. All rights reserved.

Keywords: Grain growth; Texture; Grain topology; Silicon steel; Goss grains

1. Introduction

The pronounced formation of large grains with a $\{110\}\langle 001 \rangle$ crystal orientation during annealing of silicon steel sheets has been exten-

sively investigated since the early work of Goss [1], Ruder [2], and Burwell [3]. The occurrence and orientational sharpness of the $\{110\}\langle 001 \rangle$ texture component which is also referred to as Goss orientation is of considerable interest both from a technological and from a scientific point of view. The strong Goss texture which develops by secondary recrystallization can be very sharp although it does not prevail in the texture of primary recrystallized Si steel sheet.

* Corresponding author. Tel.: +49-2116-79-2800; fax: +49-2116-79-2333.

E-mail address: chen@mpie.de (N. Chen).

As primary recrystallization, secondary recrystallization is a process of nucleation followed by grain growth. The driving force for this process is the reduction of grain boundary energy. As in primary recrystallization, the secondary recrystallization texture formation may be explained by one or both of the two competing models of *oriented nucleation* and *oriented growth*. In contrast to primary recrystallization, however, secondary recrystallization, or abnormal grain growth, stands in competition with the process of normal grain growth, which also leads to a reduction of the grain boundary energy. Abnormal grain growth can only proceed if normal grain growth is inhibited. The inhibition occurs in most cases by finely dispersed particles which pin the grain boundaries. For this case Hillert [4] has shown how particle size and distribution influence the critical grain size necessary for nucleation of secondary recrystallization. In other cases the inhibition of normal grain growth may occur by the existence of a very sharp primary texture. In this case the low angle grain boundaries between most of the grains prevent normal grain growth and only those grains with strongly deviating orientations may grow abnormally. It should be mentioned that in the case of polycrystals which do not contain any second-phase particles and show a random texture large grains will always grow more slowly than small grains and will finally join the normal grain size distribution [4,5]. Thus, in such ‘ideal’ polycrystals abnormal grain growth will never occur.

In the case of the Goss texture formation in primary recrystallized silicon steel the inhibition of normal grain growth occurs by particles (manganese sulfide or aluminum nitride particles), while texture has no serious inhibiting effect because the primary recrystallization texture is rather weak. This has already been shown by investigations of May and Turnbull [6] on high purity silicon steel where no abnormal grain growth occurred because second phase particles were absent.

Concerning the mechanism of texture formation the idea of oriented growth has been most frequently favored and two models have been proposed. The first one [7,8] suggests that CSL (coincidence site lattice) grain boundaries are

responsible for the abnormal growth of Goss grains. Statistically, Goss oriented grains in a typical primary recrystallization texture have a higher probability than other orientations to form low- Σ CSL boundaries (i.e. boundaries with a high number of lattice coincidence sites). Lin et al. [8] claimed that these boundaries have a higher mobility than others. It should be noted in this context that the CSL model has no physical meaning as such but is a geometrical concept from which possible physical mechanisms such as grain boundary dislocations or solubility of foreign atoms can be derived.

The second view on oriented growth of Goss grains is based on the assumption that high mobility is a feature of high-angle boundaries with misorientation angles between 20 to 45° [9,10]. The idea here is that the high diffusivity of these boundaries leads to quick coarsening of precipitates during annealing. The resulting large particles have a lower pinning force on the moving boundaries than smaller particles on other boundaries. Goss grains have been reported to be surrounded by a higher fraction of these high mobility grain boundaries than grains with other orientations. This unique configuration is assumed to be the reason for abnormal growth of Goss grains.

Both approaches have recently been discussed by Morawiec [11] who concluded that possible differences in grain boundary mobility might not be the sole reason for the abnormal grain growth of Goss grains. Using local orientation measurements and Monte Carlo simulations Chen et al. [12] also found that differences in the mobility alone do not seem to be sufficient for abnormal grain growth of Goss oriented crystals. Also, it is questionable whether the only statistical link between the Goss orientation and a particular grain boundary character (high angle or CSL grain boundary) is able to create a texture as sharp as the observed Goss texture.

A strong objection against either of these two theories of oriented growth is that usually only very few grains with a sharp Goss orientation are observed to start growing in the early stage of secondary recrystallization, i.e. that there is no growth competition. This observation supports the classical idea of oriented nucleation as main mechanism

of secondary recrystallization. In this case it is assumed that a grain may grow abnormally if it has a certain size advantage over the other crystals in the primary recrystallized matrix. The open problems in understanding this phenomenon are first to define the critical grain size from which on a grain may grow abnormally and second to explain how grains of a sufficient size develop in the matrix. According to Hillert [4] the critical grain size depends on the grain boundary energy, on the average grain size and on the size and distribution of the inhibiting particles. It may also be influenced by the surface energy in case that the grain is close to the free surface of the sheet. The question how a grain may reach the critical grain size has been answered in different ways. Some authors (Matsuo [13], Inokuti et al. [14]) claim the existence of large Goss oriented grains in the primary recrystallized matrix. Matsuo [13] found many Goss grains in the subsurface layer of a hot rolled silicon steel sheet. On the basis of this observation he assumed the presence of some larger Goss grains in this layer also after cold rolling and subsequent primary recrystallization. Others assume that Goss grains may be formed by coalescence of closely oriented grain clusters [Inokuti et al. [14]]. In both cases nuclei for secondary recrystallization are assumed to be created by inheritance from the hot rolled sheet.

Instead of using the grain size as a measure for a topological advantage of a grain it is, according to von Neumann [15], Mullins [16], and Hillert [4], more sensible to use the number of next neighbors of a grain. For the simple case of a two-dimensional microstructure, a grain will grow if it has more than six neighbors and shrink if it has less than six. In the three-dimensional case, no regular polyhedron with plane faces exists which fills space completely and balances the boundary tensions. Therefore, grain growth is inevitable in a three-dimensional microstructure (Smith [17]). However, also in this case the tendency remains that grains with many neighbors grow while those with few shrink. In the case of grains in a microstructure with a homogeneous grain size distribution as it is the case here, however, statistically the number of next neighbors of a grain and the grain size are approximately related by a square

function. This means that in a first approximation grain size can be used to discuss the tendency of a grain for grain growth and this approach has been mainly adapted here. Local considerations, in contrast, must be based on the number of next neighbors.

The suggestion of oriented nucleation, i.e. initial size advantage of Goss grains has until now not been systematically investigated by experiment. This is essentially due to the rareness of the nucleation event: assuming a grain size of $20 \times 20 \times 20 \mu\text{m}^3$ in the primary recrystallized matrix and of about $2000 \times 2000 \times 200 \mu\text{m}^3$ in the secondary recrystallized material (200 μm is the sheet thickness) it is clear that on 106 primary grains comes only one successful Goss grain as nucleus for secondary recrystallization. One therefore must inspect at least 106 grains in order to observe one nucleus. This points out the demand for a fast and efficient method for single grain orientation and grain size measurements.

The aim of the present study, therefore, is to quantitatively investigate the possible existence of a size advantage of Goss-oriented (or any other) grains in the subsurface layer of primary recrystallized silicon steel sheet and to check whether such orientational topology effects might play a role for abnormal grain growth in this material.

2. Experimental

Material used in this investigation was a fully primary recrystallized Fe–3% Si sheet, which was produced by two-stage cold rolling. MnS was used as inhibitor in this type of Si steel. The texture after secondary recrystallization was investigated on a sheet which was secondary annealed by heating it for 40 h up to 1000 °C under H_2 atmosphere.

Automatic crystal orientation mapping (ACOM) was performed in a JEOL 6500F field emission gun scanning electron microscope (FEG-SEM). The ACOM technique allows determination of the crystallographic texture and the microstructure in crystalline material. Local lattice orientations are measured on a regular grid by automated acquisition and processing of electron backscatter diffraction (EBSD) patterns. The microstructure can sub-

sequently be reconstructed by coloring similar orientations on the measured grid with similar colors. The FEG-SEM used in this study is distinguished by its extraordinary high beam current at high resolution. This, together with a high-speed digital CCD camera (DigiView, TSL) for the acquisition of EBSD patterns allows measuring up to 30 patterns per second and enables the measurement of very large orientation maps in an acceptable time span.

Two kinds of investigations were carried out. First, two large orientation maps, covering $2 \times 2 \times 2 \text{ mm}^2$ were measured with high resolution on the rolling plane in order to detect possible Goss grains and to check for the relationship between texture and grain size. This area contained about 6×10^4 grains. Second, a very large area on the rolling plane of two primary recrystallized samples was investigated by inspection of backscatter electron (BSE) images in order to detect all large grains. To this end two samples with an investigated area of $2 \times 14 \times 24 \text{ mm}^2$ were used. This area corresponds to about 2×10^6 grains (which were not all investigated by ACOM) and may therefore contain two potential Goss nuclei for the subsequent secondary recrystallization. ACOM measurements were carried out in the areas surrounding all inspected large grains. By this method the orientation and the occupied areas of all large grains were determined. Two rules were used to define what was counted as a *large grain*: First, the grain diameter had to be larger than $40 \mu\text{m}$, the average diameter of all matrix grains amounted to about $20 \mu\text{m}$. Second, the grain size had to be much larger than that of the immediate neighbor grains.

All ACOM measurements were carried out in the subsurface layer ($s = 0.8$) of the samples in the rolling planes (formed by the rolling direction (RD) and transverse direction (TD)). The parameter s is defined by $s = a/(d/2)$, where a is the distance of the inspected area from the center layer and d the sheet thickness.

From the measured crystal orientations pole figures and orientation distribution functions of the large grains were calculated. For comparison the global texture was calculated from X-ray pole fig-

ure measurements carried out with a Siemens D500 X-ray texture goniometer.

The texture results will be discussed in the following in terms of the typical texture fibers found in recrystallized silicon steel. These are namely the α_{bcc} -fiber (fiber axis $\langle 110 \rangle$ parallel to the rolling direction including major components $\{001\}\langle 110 \rangle$, $\{1\bar{1}2\}\langle 110 \rangle$, and $\{111\}\langle 110 \rangle$), the γ -fiber (fiber axis $\langle 111 \rangle$ parallel to the normal direction including major components $\{1\bar{1}1\}\langle 110 \rangle$ and $\{11\bar{1}\}\langle 112 \rangle$) and the η -fiber (fiber axis $\langle 001 \rangle$ parallel to the rolling direction including major components $\{001\}\langle 100 \rangle$ and $\{011\}\langle 100 \rangle$).

3. Experimental results

Fig. 1 shows the orientation distribution function (ODF) determined by X-ray diffraction. It reveals that the texture in the investigated subsurface layer is dominated by a weak γ -fiber and a texture component on the η -fiber which is about 15° rotated about the rolling direction from the cube orientation. A minor α -fiber component at the 45° rotated cube orientation can also be observed. Fig. 1 also reveals that the exact Goss component is rather weak in the primary recrystallized specimen. Fig. 2 shows the ODF after secondary recrystallization. The texture shows a sharp Goss component with a full width half maximum (FWHM) of about 10° .

The grain size and grain orientation of a large number of grains (about 60 000) was determined by ACOM. The grain size distribution obtained from these measurements is shown in Fig. 3. The average grain size is $17.3 \mu\text{m}$ and the grain size distribution can be fitted with good precision to the two-parametrical log-normal distribution (Feltham [18]). Naturally, the only one-parametrical Hillert [4] or Rayleigh [19] distributions do not give a similarly good fit.

The correlation between grain size and grain orientation is presented in Fig. 4a in form of a graph which displays for every grain its angular deviation to the exact Goss orientation over its grain size in μm^2 . The gray value at each position in the graph corresponds to the number of grains



Fig. 1. Orientation distribution function of primary recrystallized silicon steel in the form of $\phi_1=\text{constant}$ sections using $\Delta\phi_1=5^\circ$ steps between the sections. The texture was determined by measuring the four incomplete pole figures {110}, {200}, {112}, and {103} in the range of the pole distance between 0° and 85° using Mo $K_{\alpha 1}$ x-radiation and deriving the orientation distribution function from it using spherical harmonics. The measurement was conducted in the layer $s = 0.8$ (see text).

that show similar parameters. It is visible from this graph that some grains have sizes larger than $40\ \mu\text{m}$ but there is no apparent tendency of these grains to be close to Goss orientation. The two solid lines that have been drawn in the graph mark the limit for a possible Goss nucleus with a certain size advantage. The horizontal line indicates an angular deviation of 10° from the exact Goss orientation which corresponds to the observed sharpness of the final texture. The vertical line indicates the grain size of grains which have a diameter two times larger than the average grain size. All grains right and below these lines fulfill the criteria for a Goss grain nucleus. Obviously there are only two grains in this area while several non-Goss oriented grains have large diameters.

As was already mentioned in the introduction the number of next neighbors of a grain is a more

sensible measure to evaluate a topological advantage of a grain than the grain size. However, the number of neighbors is more difficult to determine and appropriate algorithms are not included in the commercial ACOM software used here (OIM3 of TSL). Therefore a computer program was developed that determines for every grain in an orientation map the number of next neighbors. An exported data file of the OIM software containing all measurement information (location and orientation of each measurement point) serves as input for the developed algorithm. In a first step, the program uses a recursive algorithm to determine all grains and assign them a unique grain ID. To this end the misorientation of all neighbor points of a given point are checked. If the misorientation angle is less than a predefined value (for example 2°) the neighbor point is considered to be within the same

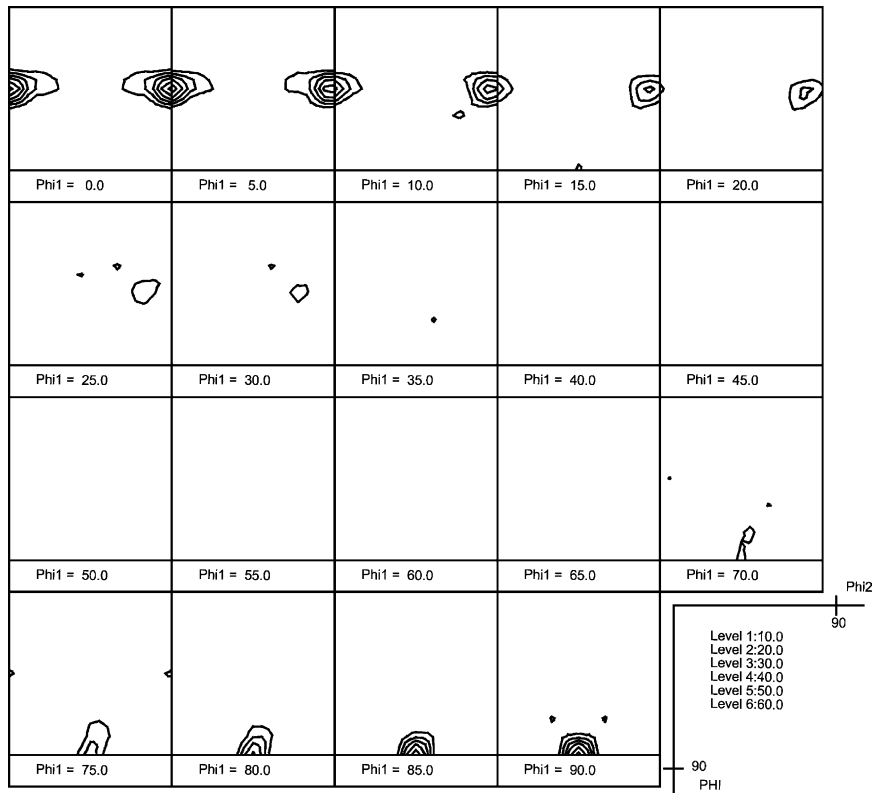


Fig. 2. Orientation distribution function after secondary recrystallization. The measurement parameters are the same as Fig. 1.

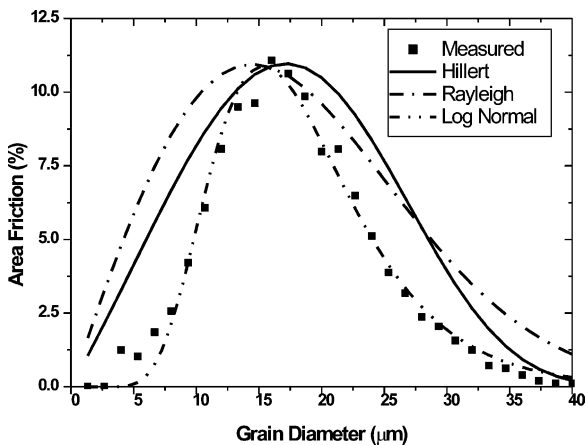


Fig. 3. Grain size distribution determined from ACOM measurements of a large area (4 mm × 2 mm) of a primary recrystallized sample.

grain, otherwise it is in a new grain. In case the point is in the same grain the same algorithm is repeated until all points belonging to one grain are found. After all grains in the OIM map have been detected a second algorithm now simply counts the number of next neighbors of each grain by comparing their grain IDs. The quaternion method is used for the calculation of misorientations in order to speed up the algorithm. On an AMD1000 GHZ computer it takes about 35 s to finish the calculation for a map of 10^6 points. Only some very small grains and grains located on the border of the map are overlooked by the algorithm. The results of these calculations are displayed in Fig. 4b in a similar way as in Fig. 4a. For every grain one point displays its angular deviation to the Goss orientation over its number of next neighbors. The gray value represents the number of grains that fall onto the same position in the graph.

Most grains have less than 13 neighbors with a

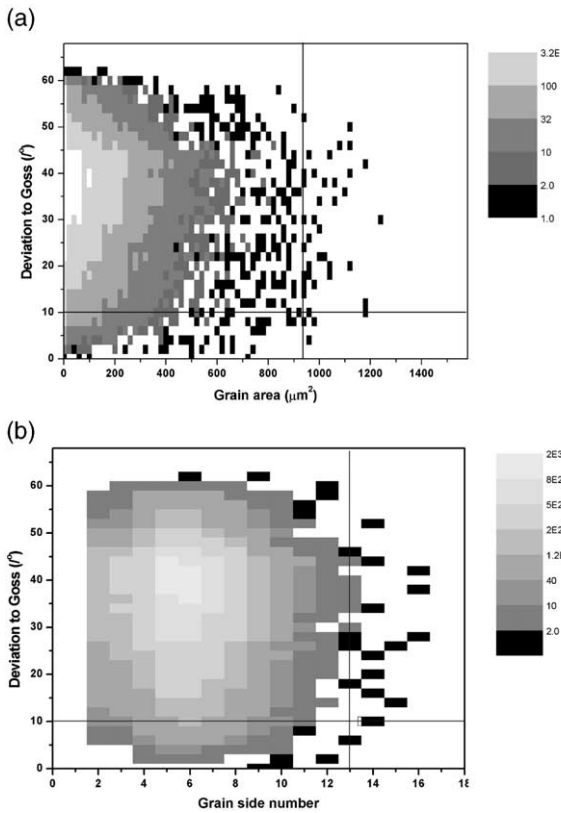


Fig. 4. Correlation between grain topology and angular deviation from the Goss orientation (all data are calculated from an ACOM measurement of a large area (4 mm × 2 mm) of a primary recrystallized sample). The gray value of a given position corresponds to the number of grains that show this particular combination of topology and Goss deviation. Points which correspond to only one single grain are displayed in black on a white background. Do not confuse this background with the white area in the center of the graphic which corresponds to areas with maximum number of grains. (a) Correlation between grain area (in μm^2) and angular deviation to Goss (in $^\circ$). (b) Correlation between number of next neighbors and angular deviation to Goss (in $^\circ$).

maximum of grains owing five or six neighbors as it is expected for a stable two-dimensional structure. The largest number of next neighbors is 16 and there are three grains corresponding to this number. However, their deviation from the Goss orientation is for all of them larger than 25° . There is only one grain with a Goss orientation deviation of less than 10° and a number of next neighbors larger than 14 in this graph. As for the grain size no tendency of grains with a high number of next

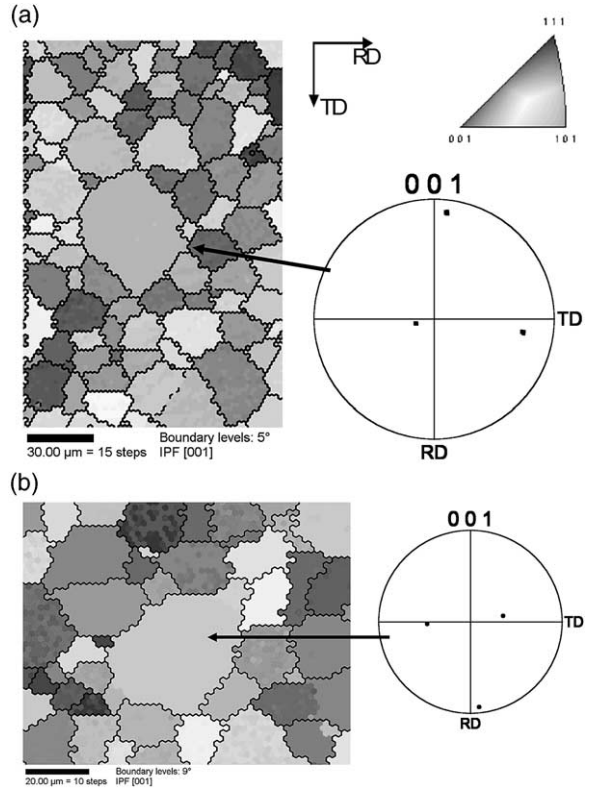


Fig. 5. Crystal orientation maps of large grains in the primary recrystallized silicon steel. The gray value is chosen according to the crystal direction parallel to the normal direction of the sheet. The orientation of the large crystal is displayed as (001) pole figure. (a) Large non-Goss grain on the η -fibre. (b) Goss grain with many neighbors.

neighbors to be close to the Goss orientation is visible.

Fig. 5a shows an example of the local orientation measurements that were systematically conducted around all large grains. The pole figure projection shows that this particular grain is close to the cube orientation $\{001\}\langle 100 \rangle$. The crystal orientation and size of all inspected 22 large grains are presented in Fig. 6a, the corresponding next-neighbor graph in Fig. 6b. Fig. 6a shows that the area of most of the large grains is in the range between 1200 and 3000 μm^2 corresponding to a diameter of 40–60 μm . The area of the largest grain is 4562 μm^2 , i.e. its diameter is about 80 μm which is about four times larger than the average grain size. A comparison between Figs. 6a and 6b

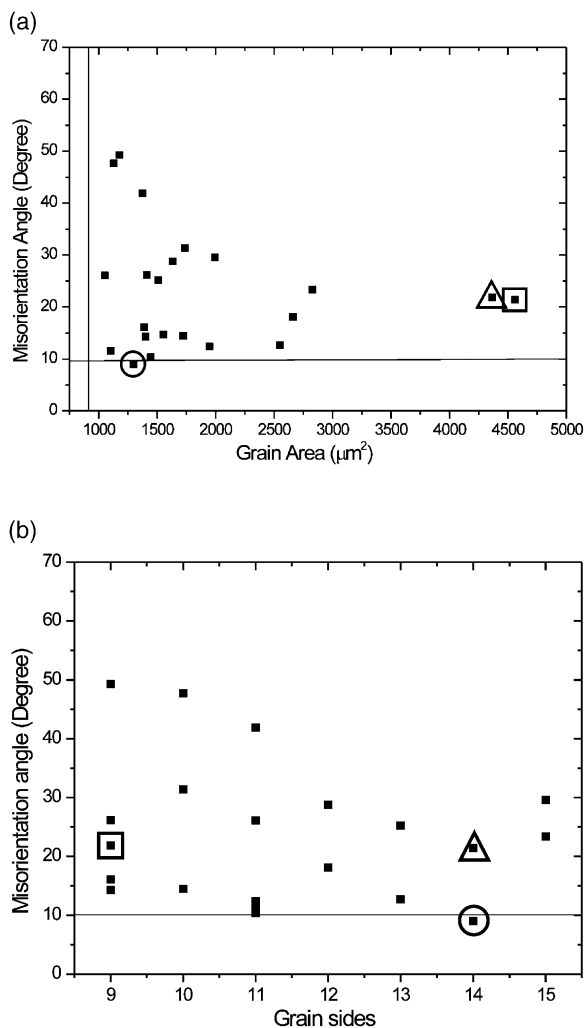


Fig. 6. Correlation between grain topology and angular deviation to the Goss orientation for large grains (measurements conducted on different areas of two samples). The same three grains are marked in both graphs. (a) Correlation between grain area (in μm^2) and angular deviation to Goss (in $^\circ$). (b) Correlation between number of next neighbors and angular deviation to Goss (in $^\circ$).

reveals that the large grains are not necessarily those with many neighbors and vice versa. One quite small grain ($1296 \mu\text{m}^2$ (Fig. 5b)), marked by a circle in the graph, actually has a very large number of neighbors (14) and therefore probably a high tendency to grow. Since it is also the only grain with an angular deviation to Goss of smaller than 10° this grain actually might be a Goss nucleus.

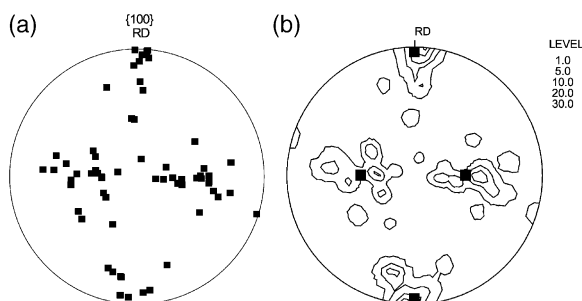


Fig. 7. (a) Discrete $\{100\}$ pole figure of all large grains. (b) Continuous $\{100\}$ pole figure of all large grains, weighted by grain size.

The orientation distribution of all investigated 22 large grains is shown in Fig. 7 in the form of $\{100\}$ pole figures and in Fig. 8 in the form of an orientation distribution function. The left hand side of Fig. 7 shows the $\{100\}$ projection points of the orientations of the large grains without considering the actual size of each grain while the right hand side pole figures are weighted by the grain size. Figs. 7 and 8 substantiate that most large grains have an orientation close to the η -fiber. However, the distribution of the intensity along the η -fiber is not homogeneous. According to Fig. 8, a maximum orientation density occurs at $\phi_1=0^\circ$, $\phi_2=33^\circ$, $\phi_3=0^\circ$ and at $\phi_1=0^\circ$, $\phi_2=57^\circ$, $\phi_3=0^\circ$ (symmetrically equivalent to the first). The intensity of the exact Goss orientation at $\phi_1=0^\circ$, $\phi_2=45^\circ$, $\phi_3=0^\circ$ is relatively low. The actual maxima on the η -fiber are rotated 12 – 13° around the rolling direction of the sheet from the Goss orientation. In contrast to the texture of *all* grains given in Fig. 1 practically no γ - or α -fiber crystals are found among the large grains.

4. Discussion

The ODF obtained by X-ray diffraction in the $s = 0.8$ layer shown in Fig. 1 is a typical sub-surface texture of a primary recrystallized silicon steel. It is characterized by a weak γ -, η -, and α -fiber. While the occurrence of a pronounced γ -fiber and of a minor α -fiber is well known from textures of primary recrystallized body-centered cubic metals, the η -fiber is usually less pronounced in such

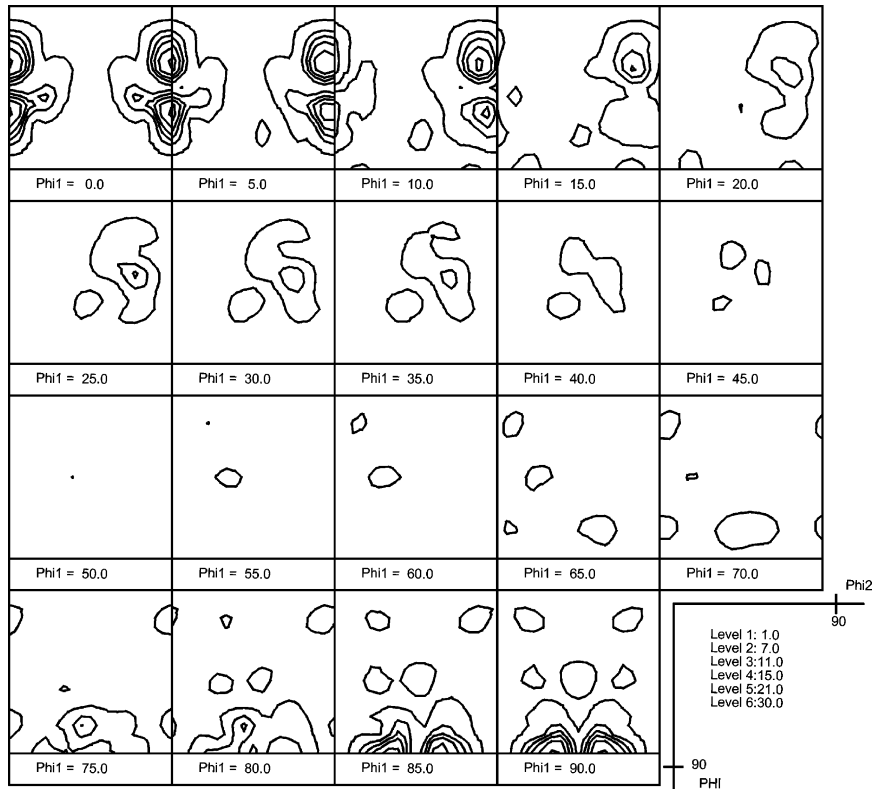


Fig. 8. ODF of large grains calculated from orientation and size of large grains.

material [14,20–24]. The η -fiber is usually found in body-centered metals if the sheet has undergone substantial friction and sub-surface shear during hot rolling. Typically, it appears stronger in steels which are alloyed with elements enlarging the high-temperature stability of the ferrite phase [25]. Depending on the further strain and annealing path, the η -fiber becomes more or less pronounced. Mishra et al. [26] reported for a high-permeability grain-oriented Si steel (using only one stage of cold reduction) a strong η -fiber with a maximum close to $\{013\}\langle 100 \rangle$ ($\varphi_1, \phi, \varphi_2$) = (0°, 18.4°, 0°) in the $s = 0.8$ layer. Fig. 1 shows that the exact Goss component at ($\varphi_1, \phi, \varphi_2$) = (0°, 45°, 0°) is rather weak in the primary recrystallized sample. This observation is in agreement with previous work [26].

In case that topology, i.e. number of next neighbors respectively grain size plays the dominant role during secondary recrystallization and assuming

further that mobility as well as energy aspects are homogeneous throughout the microstructure, the grain with the largest number of neighbors (which might be one of the largest grains) in the inspected subsurface layer of the primary recrystallized steel should be close to the Goss orientation. The ODF of the secondary recrystallized material shows a maximum deviation from the Goss orientation of about 10° and this should be the same for the grains serving as nuclei.

From the data presented in Fig. 4 no tendency is visible that grains are the closer to the Goss orientation the larger they are or the more neighbors they have. Quite the contrary, Fig. 4 shows that large grains, respectively grains with many neighbors show a similar distance to the Goss orientation as the smaller grains or grains with few neighbors.

For the 22 very large grains (Fig. 6) which all have orientations close to the η -fiber the maximum

of the orientation distribution function shows 12° deviation from the precise Goss component. It is therefore impossible to obtain a sharp Goss texture from these grains. However, one suitable Goss grain nucleus displayed in Fig. 5b and marked with a circle in Fig. 6 has been detected. Indeed, this grain is not under the very largest grains but it is a grain with a high number of neighbors, meaning that this grain is situated in an area of the primary recrystallized material with relatively small average grain size. In contrast, the two largest grains, marked by a triangle and a square in Fig. 6 have angular deviations to the Goss orientation of 21.9° and 21.4° and therefore, obviously, cannot act as typical nuclei for the sharp secondary recrystallization Goss texture. Also, one of these grains has a much smaller number of next neighbors (9) and should therefore have a comparatively low tendency to grow. The other, however, has the same number of neighbors as the possible Goss nucleus and it is not clear why this grain should, in comparison to the possible Goss nucleus, not be able to grow. It must be mentioned that the growth behavior of these areas has not been investigated yet due to experimental difficulties. It is therefore up to now not possible to make a clear statement on the importance of grain topology for the development of the Goss texture.

A comparison of Figs. 4 and 6 reveals that for a *statistical* evaluation of the topology effect on grain growth the grain size may be a reasonable measure because in a homogeneous microstructure grain area and number of next neighbors (i.e. the grains circumference) are approximately related by a square function. For a detailed discussion of *particular* grains, however, this statistically expected relationship between grain size and number of next neighbors does not need to be correct and it is very important to determine both values in order to detect possible Goss grain nuclei.

5. Conclusions

It was investigated whether a topological advantage (either size or number of next neighbors) of Goss oriented grains in the primary recrystallized microstructure could be responsible for the sharp

Goss texture developing during secondary recrystallization in silicon transformer steel. Two types of measurements were carried out by automatic crystal orientation measurements (ACOM) in a field emission gun scanning electron microscope (FEGSEM) on a subsurface layer of a primary recrystallized sample. First the size, number of next neighbors and orientation distribution of a large amount of grains was determined. No tendency for large grains or grains with many next neighbors to be close to Goss grains was found. Second, the orientation distribution of particularly large grains was investigated. The large grains were mainly located on the η -fiber in Euler orientation space but the Goss orientation was only weakly occupied. The grains which were closest to the Goss orientation were not particularly large while the largest grains were more than 20° away from the Goss orientation. However, one grain which was close to the Goss orientation, although not very large, showed a particularly high number of next neighbors and might therefore be a possible Goss nucleus. Though, also some grains with a high deviation from the Goss orientation showed the same or even higher number of next neighbors and it is not clear why these grains should not also be able to act as a nuclei for secondary recrystallization. It can be concluded that an inherited topology effect alone cannot explain the dominance of the Goss texture during secondary recrystallization of silicon steel. Alternatively it might be that no relevant Goss nucleus has been observed yet. This assumption is supported by the extreme rareness of these grains because only one grain out of 10^6 in the primary recrystallized structure will grow during secondary recrystallization.

References

- [1] Goss NP. Trans Am Soc Metals. 1935;23:511.
- [2] Ruder WE. Asm 1935;23:534.
- [3] Burwell JT. Trans. AIME 1940;140:353.
- [4] Hillert M. Acta Metall 1965;13:227.
- [5] Srolovity DJ, Grest GS, Anderson MP. Acta Metall 1985;33:2233.
- [6] May JE, Turnbull D. Trans. AIME 1958;769:781.
- [7] Shimizu R, Harase J. Acta Metall 1989;37:1241.
- [8] Lin P, Palumbo G, Harase J, Aust KT. Acta Mater 1996;44:4677.

- [9] Hayakawa Y, Szpunar JA. *Acta Mater* 1997;45:1285.
- [10] Rajmohan N, Szpunar JA, Hayakawa Y. *Acta Mater* 1999;47:2999.
- [11] Morawiec A. *Scripta Metall* 2000;43:275.
- [12] Chen N, Zaeferrer S, Lahn L, Günther K, Raabe D. In: Lee S, editor. *Proceedings of the 13th International conference on Textures of Materials (ICOTOM 13)*. Seoul, South Korea, 2002:949.
- [13] Matsuo MI. *ISIJ International* 1989;29:809.
- [14] Inokuti, Maeda C, Itoh Y, Shimanaka H. *ICOTOM6*. Tokyo, 1981:948.
- [15] Von Neumann J. *Metal interfaces*. Cleveland: American Society for Metals, 1952:108.
- [16] Mullins WW. *Journal of Applied Physics* 1956;27:900.
- [17] Smith CS. *Metal Interfaces*. Cleveland: ASM, 1952:65
- [18] Feltham P. *Acta Metall* 1957;5:97.
- [19] Louat NP. *Acta Metall* 1974;22:721.
- [20] Därmann C, Mishra S, Lücke K. *Acta Metall* 1984;32:2185.
- [21] Schlippenbach UV, Emren F, Lücke K. *Acta Metall* 1986;34:1289.
- [22] Hutchinson WB. *Int. Mat. Rev* 1984;29:25.
- [23] Ushioda K, Hutchinson WB, Agren J, Schlippenbach UV. *Mat. Sci. and Techn* 1986;2:807.
- [24] Hölscher M, Raabe D, Lücke K. *Steel Research* 1991;62:567.
- [25] Raabe DL, Lücke K. *Scripta Metall* 1992;26:1221.
- [26] Mishra S, Därmann C, Lücke K. *Metal Trans* 1986;17A:1301.